Supporting information

Synthesis of spin-labeled riboswitch RNAs using convertible nucleosides and DNA-catalyzed RNA ligation

Lea Büttner, Jan Seikowski, Katarzyna Wawrzyniak, Anne Ochmann, Claudia Höbartner

Research Group Nucleic Acid Chemistry, Max Planck Institute for Biophysical Chemistry,
Am Fassberg 11, 37077 Göttingen, Germany

Table of contents

Table S1. Unmodified RNAs prepared by solid-phase synthesis or in vitro transcription.

No	5'-Sequence-3'	m.w. calcd.	m.w. found[a]
10	GACGUCGGA	2893.8	2893.1
10'	UCCGACGUC	2790.7	2789.7
11	AAGUCUCAUGUACUA	4720.9	4720.1
11'	UAGUACAUGAGACUU	4760.9	4760.8
12	GACGUCGGAAGACGUCAGUA	6469.0	6468.5
12'	UACUGACGUCUUCCGACGUC	6279.8	6279.5
13	pppGAUCAAGUGUAGUAUCU	5652.2	5651.4
15	pppGAUGUUCUAGCGCCGGA	5579.2	5578.2
17	pppGACCUCGCAUCGUG	4661.6	4661.9
18'	CACGAUGCGAGGUCUACUGACGUCUUCCGACGUC	10826.5	10827.2
20	GUUCCCGAAAGGAUGGUGGAAUCACCA	8695.3	8694.3
21	pppGAUGCCUUGUAACCGAAAGGGGGAAU	8670.1	8670.5
22	UUCUUAUCAAGAGAAGCA	5724.5	5725.1
23	pppGAGGGACUGGCCCGACGAAGCUUCAGCAACCGGUGUAAUGGCGAUCAGCCAU	17048.1	n.d.[b]
25	pppGAGGGACUGGCCCGACGAAGCUUCAGCAACCGGUGUAAUGGCGAUCAGCCAU GACCAAGGUGCUAAAUCCAGCAAGCUCGAACAGCUUGGAAGAUAAGAA	32640.6	n.d.[b]

[a] by ESI-MS. [b] m.w. not determined by ESI-MS, correct length of transcript was confirmed by comparison with length standards on PAGE

Table S2. Sequences of 9DB1* deoxyribozymes

No	5'-Sequence-3'
D1	TACTACACTTGAT**GGATCATACGGTCGGAGGGGTTTGCCGTTTA**CCGACGTC
D2	TCCGGCGCTAGAACAT**GGATCATACGGTCGGAGGGGTTTGCCGTTTA**AGTACATGAGACTTCC
D3	CACGATGCGAGGT**GGATCATACGGTCGGAGGGGTTTGCCGTTTA**ACTGACGTCTTCCGAC
D4	TCGGTTACAAGGCAT**GGATCATACGGTCGGAGGGGTTTGCCGTTTA**GGTGATTCCACCATCCTTTCGG
D5	GCTTCGTCGGCCAGTCCCT**GGATCATACGGTCGGAGGGGTTTGCCGTTTA**GCTTCTCTTGATAAG

Splints for ligation with T4 DNA ligase

S1 GCGCTAGAACATCTAGTACATGACAC for (**11**+p**15**)

S2 ACGATGCGAGGTCTACTGACGTCTTCCG (for **12**+p**17**)

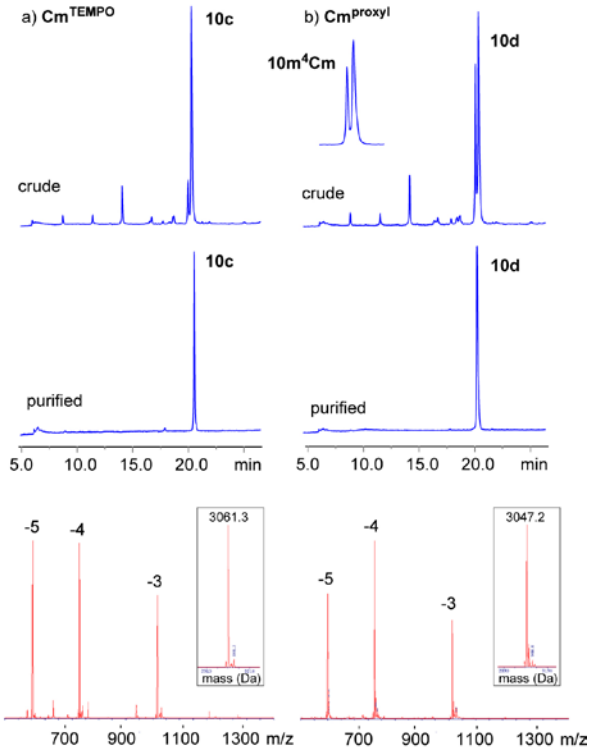

Figure S1. Anion exchange HPLC analysis of crude and purified spin-labeled 9-mer RNAs **10**, containing Cm^{TEMPO} and Cm^{proxyl} labels, and characterization by ESI-MS. **10c**: m.w. calcd. 3061.8, found 3061.3; **10d**: m.w. calcd. 3047.8, found 3047.2.

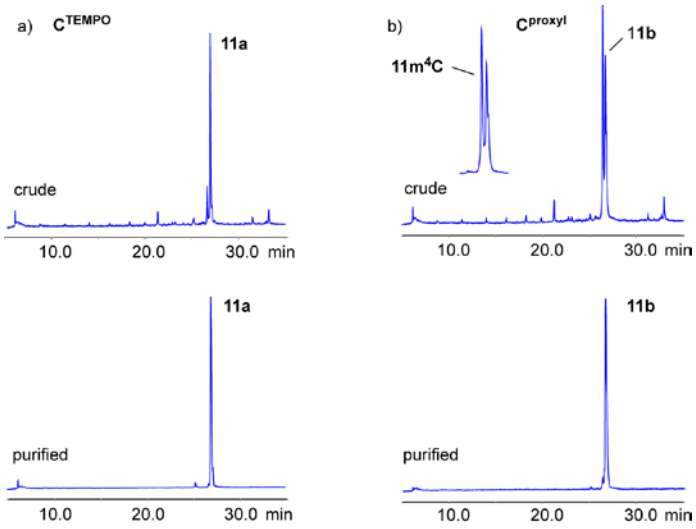

Figure S2. Anion exchange HPLC analysis of crude and purified spin-labeled 15-mer RNAs **11a** and **11b**, containing C^{TEMPO} and C^{proxyl} labels.

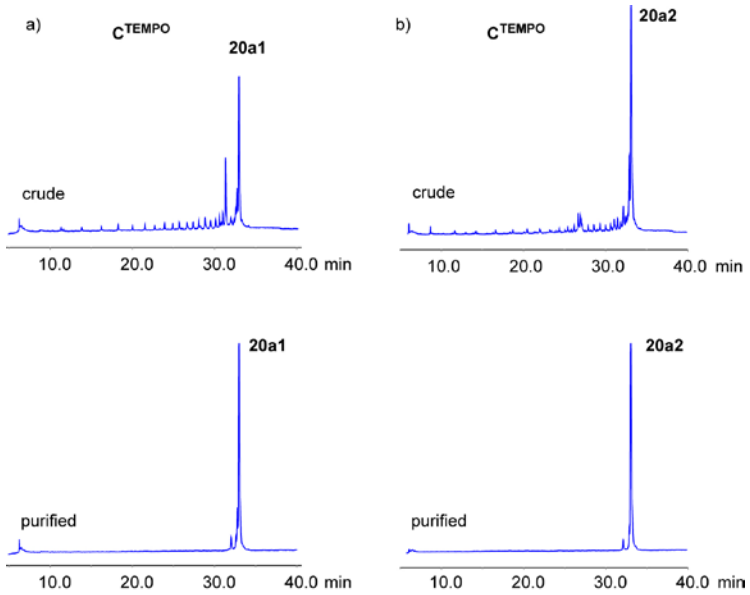

Figure S3. Anion exchange HPLC analysis of crude and purified spin-labeled SAM-III riboswitch fragments **20**, containing C^{TEMPO} labels.

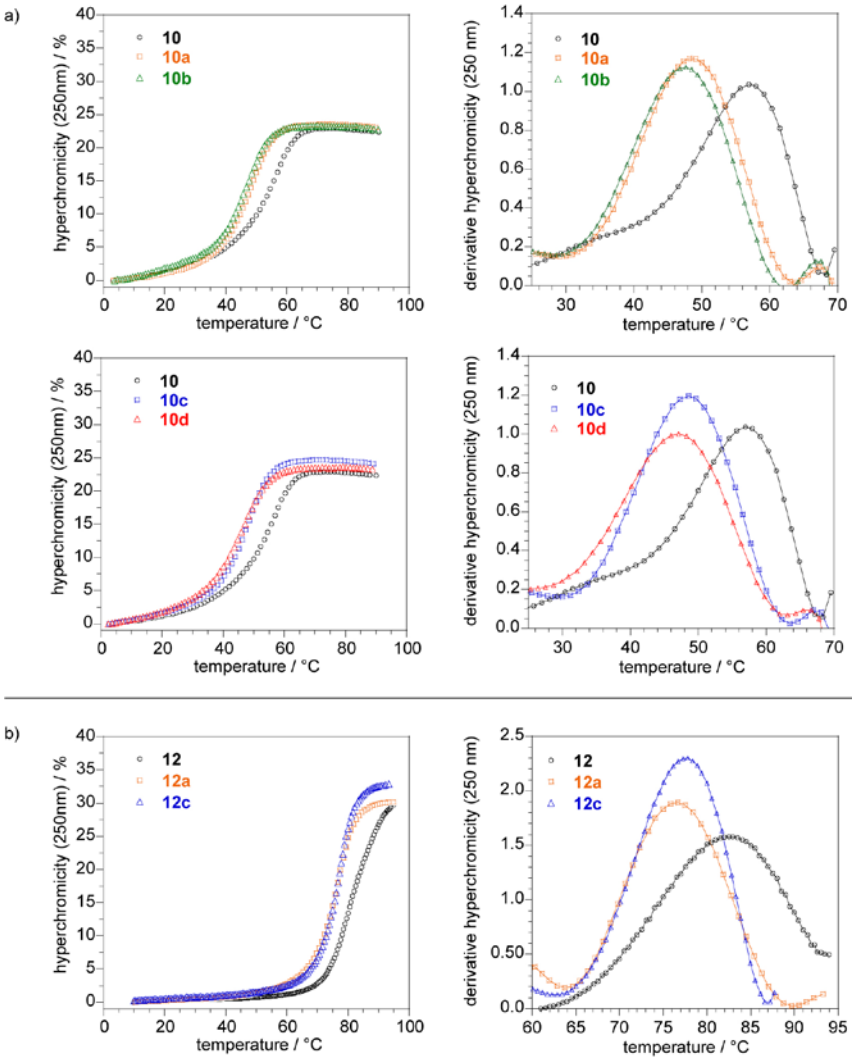

Figure S4. Melting curves of a) 9-bp duplexes 10/10'; b) 20-bp duplexes 12/12'. (left: hyperchromicity at 250 nm, right: derivative of hyperchromicity at 250 nm). RNA concentration: 4 µM, in 10 mM potassium phosphate, pH 7.0, 150 mM NaCl.

Table S3. Concentration-dependent melting temperatures for duplexes **11**/**11'**.

C(**11** unmod)		C^{TEMPO} (**11a**)		C^{proxyl} (**11b**)		Cm^{TEMPO} (**11c**)		Cm^{proxyl} (**11d**)	
conc[a] / µM	Tm / °C	conc / µM	Tm / °C	conc / µM	Tm / °C	conc / µM	Tm / °C	conc / µM	Tm / °C
1.7	62.4	1.7	57.4	1.9	56.5	1.5	58.4	1.6	57.7
3.7	**64.0**	2.4	**58.7**	2.8	**57.9**	3.5	**59.1**	3.5	**58.4**
4.9	64.2	5.7	59.3	6.0	58.5	7.5	60.1	7.3	59.2
6.4	64.5	7.3	59.5	7.7	58.8	9.3	60.1	8.9	59.6
9.4	64.8	9.0	60.3	9.9	59.5	10.9	60.9	9.2	59.8
17.1	66.2	17.8	61.6	18.0	60.7	19.8	62.2	16.8	61.0
25.0	67.2	26.4	62.4	26.4	61.6	32.2	63.5	28.6	61.9

[a] concentration calculated from absorbance at 260 nm at Tm. bold values are given in Table 2.

Table S4. Thermodynamic parameters for duplexes **11**/**11'**.

No	label	ΔH° kcal.mol^{-1}	ΔS° cal.(mol.K)$^{-1}$	ΔG°$_{298}$ kcal.mol^{-1}
11	-	-135	-373	-23.8
11a	C^{TEMPO}	-129	-361	-21.4
11b	C^{proxyl}	-125	-351	-20.8
11c	Cm^{TEMPO}	-133	-373	-22.1
11d	Cm^{proxyl}	-148	-419	-23.2

(error: ΔH°, ΔS° 5-10%, ΔG° 2-5%)

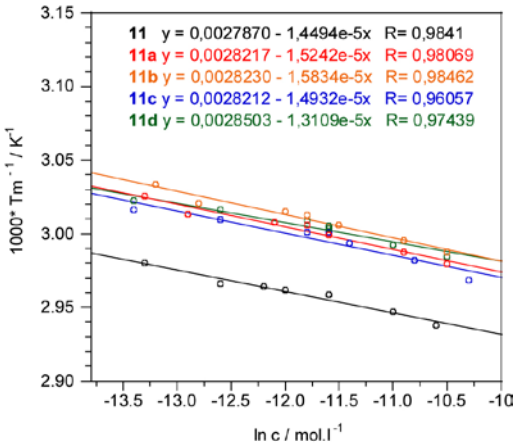

Figure S5. Van't Hoff plot for thermal analysis of 15-mer RNA duplexes **11**/**11'**. Analysis of the bimolecular melting transition of the non-selfcomplementary duplex follows equation (1); thermodynamic parameters are obtained from slope and intercept of the linear regression of the data in the plot of ln(c) vs $1/T_m$.

equation (1): $$\frac{1}{T_m} = \frac{R}{\Delta H^\circ} \ln c_{tot} + \frac{\Delta S^\circ - R \ln 4}{\Delta H^\circ}$$

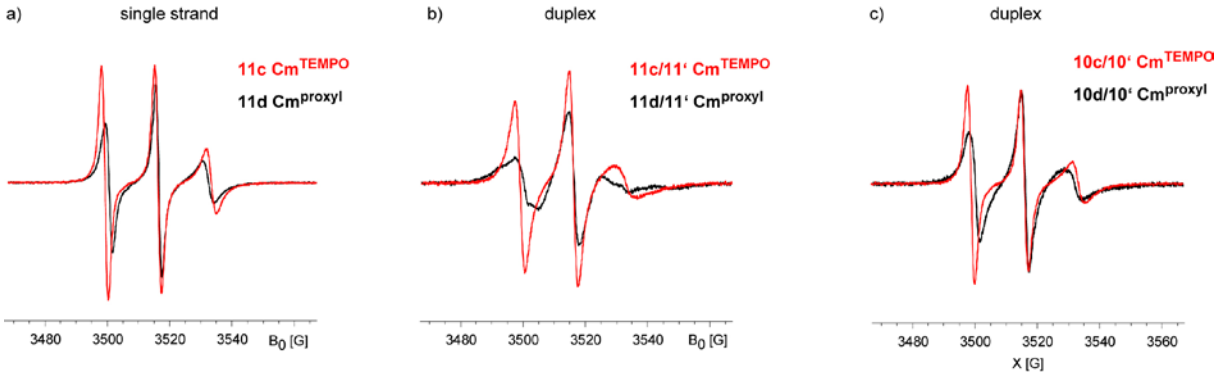

Figure S6. Comparison of CW-EPR spectra TEMPO and proxyl-labeled RNAs in single strand and duplex conformations. a) single-strands of RNA **11c** and **11d**; b) duplexes **11c**/**11'**, **11d**/**11'**, c) duplexes **10c**/**10'**, **10d**/**10'**. 200 µM spin-labeled RNA (1.5 equiv of complementary strand for duplexes), in 2.5 mM potassium phosphate, pH 7.0, 30 mM NaCl, room temperature.

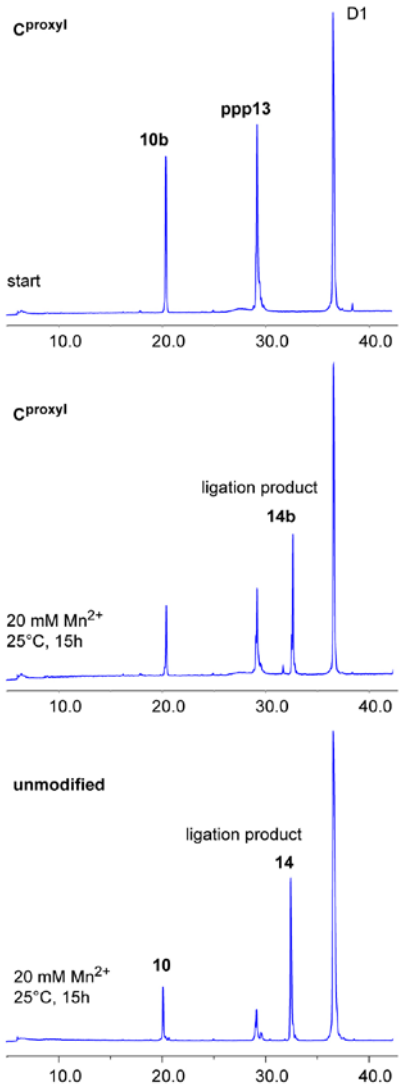

Figure S7. 9DB1*-catalyzed ligation of 9-mer **10**/**10b** and 17-mer **13**. 15 µM each RNA substrate, 50 mM HEPES, pH 7.5, 20 mM $MnCl_2$, 150 mM NaCl, 2 mM KCl, 25°C, 15 h.

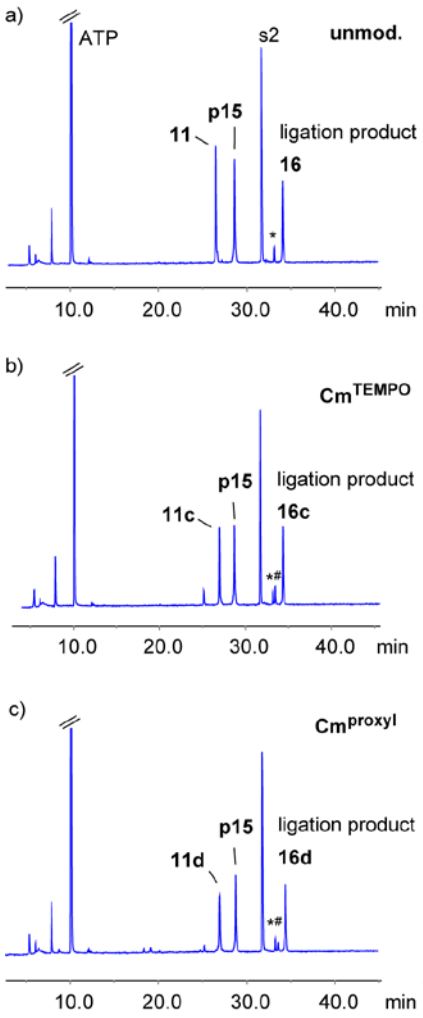

Figure S8. T4 DNA ligase-catalyzed splinted ligation of 15-mers **11**, **11c**, **11d** and 17-mer **15**. 15 µM each RNA substrate, 1x T4 DNA ligase buffer, 0.5 u/µLT4 DNA ligase, 37°C, 6 h. * byproduct produced with unmodified RNA (likely a cyclization product), # reduced byproduct from spin-labeled RNAs.

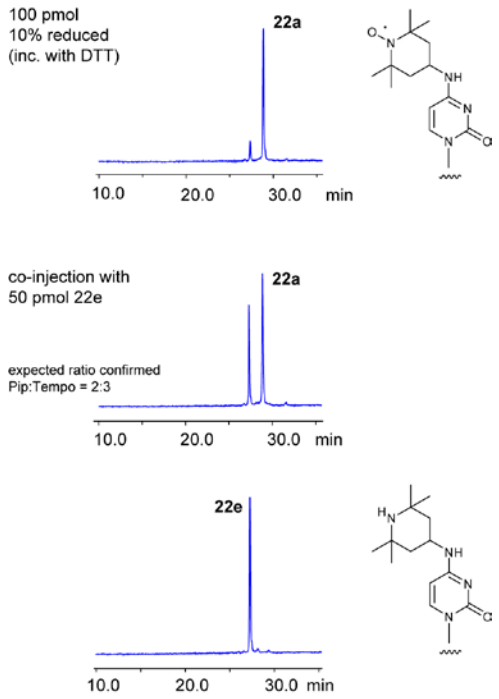

Figure S9. HPLC analysis of TEMPO reduction. Comparison with authentic piperidine-substituted RNA.

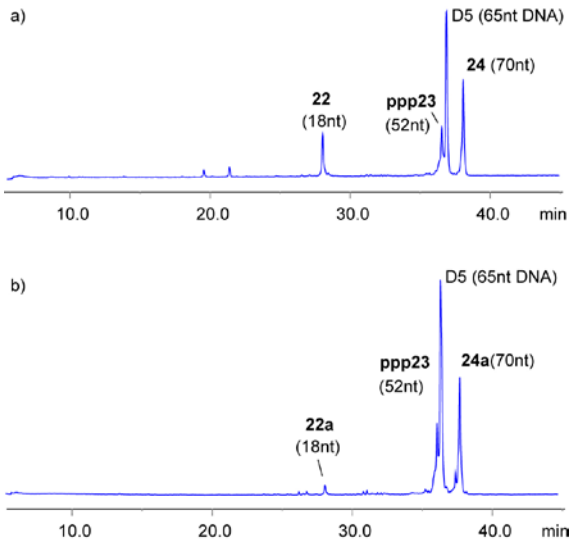

Figure S10. HPLC analysis of 9DB1*-catalyzed ligation of **22**/**22a** to **23** to generate the first 70 nt of the SAM-I riboswitch sequence. (in b) the transcript **23** was used in 1.5-fold excess over the spin-labeled RNA **22a**)

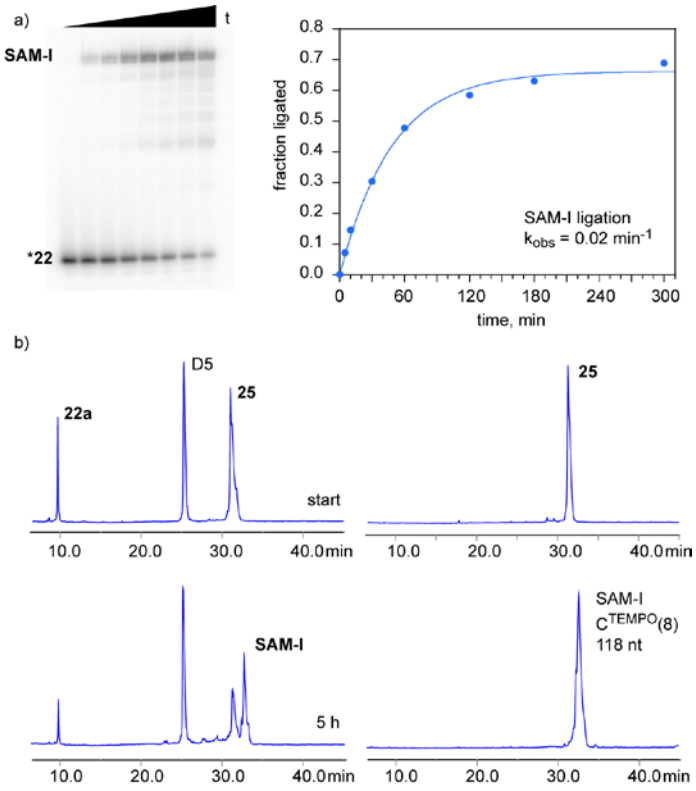

Figure S11. a) Kinetics of 9DB1*-catalyzed synthesis of SAM-I RNA using 5'-^{32}P-labeled **22** and transcript **25**. 10 µM RNA, 20 mM $MnCl_2$, 50 mM HEPES pH 7.5, 150 mM NaCl, 2 mM KCl, 37°C. b) HPLC analysis of preparative ligation (start and after 5 h). right: analytical HPLC traces of transcript **25** and isolated ligation product, full-length spin-labeled SAM-I RNA (isolated yield: 30%).

NMR spectra of new compounds

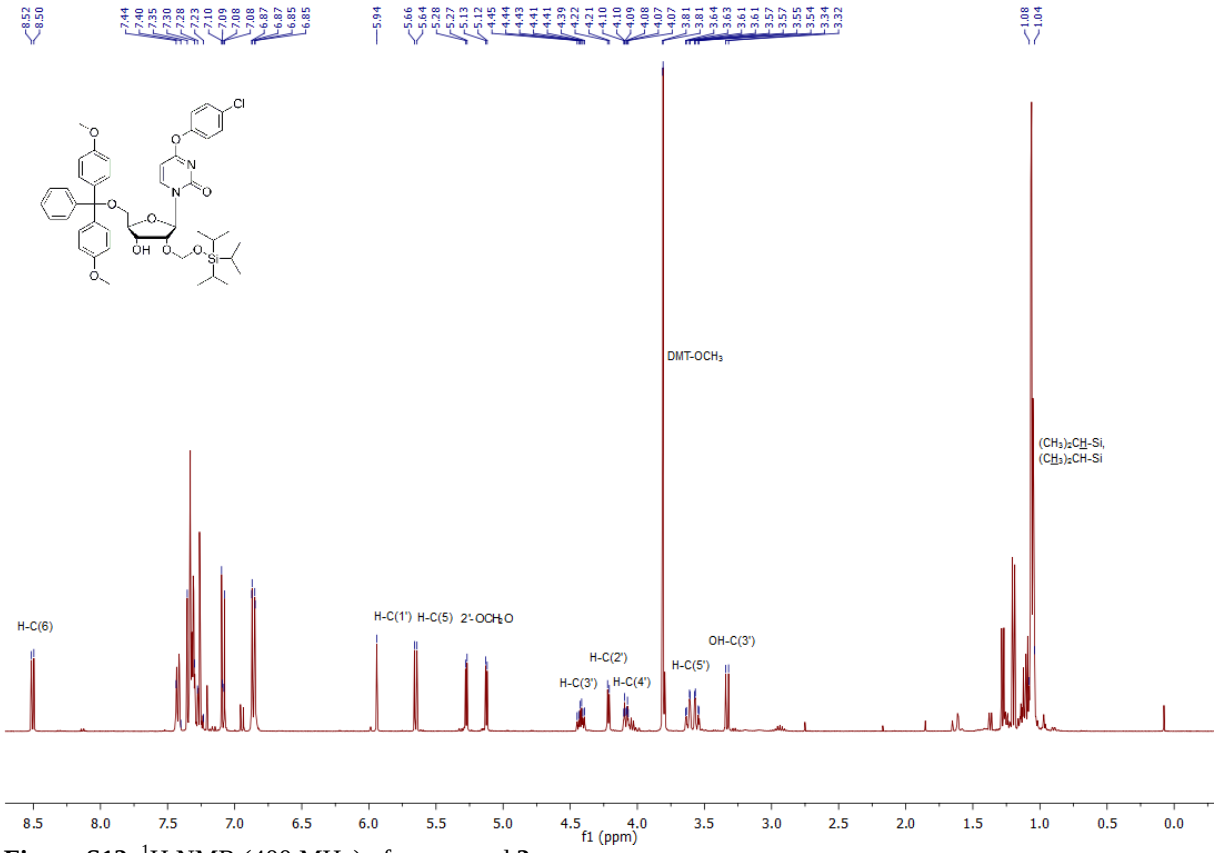

Figure S12. ^{1}H NMR (400 MHz) of compound **3**.

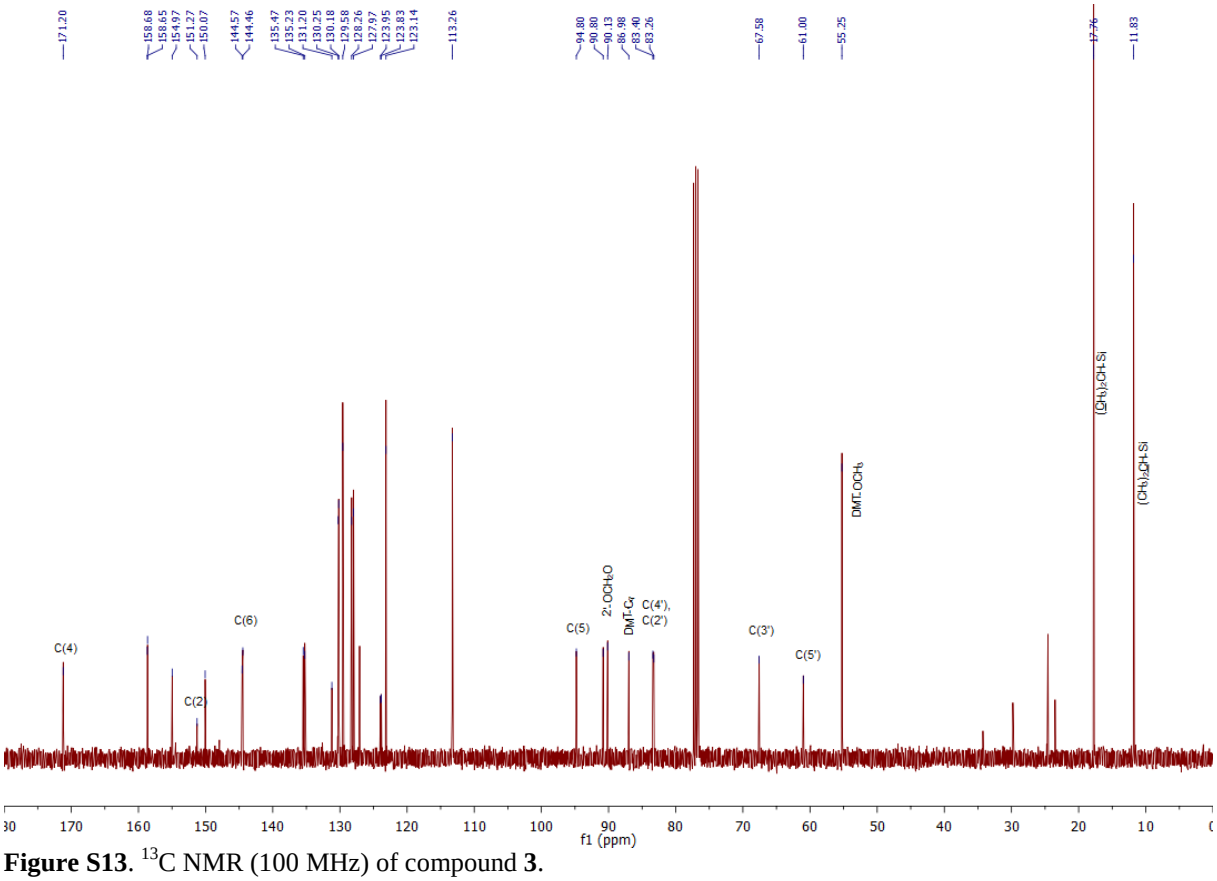

Figure S13. ^{13}C NMR (100 MHz) of compound **3**.

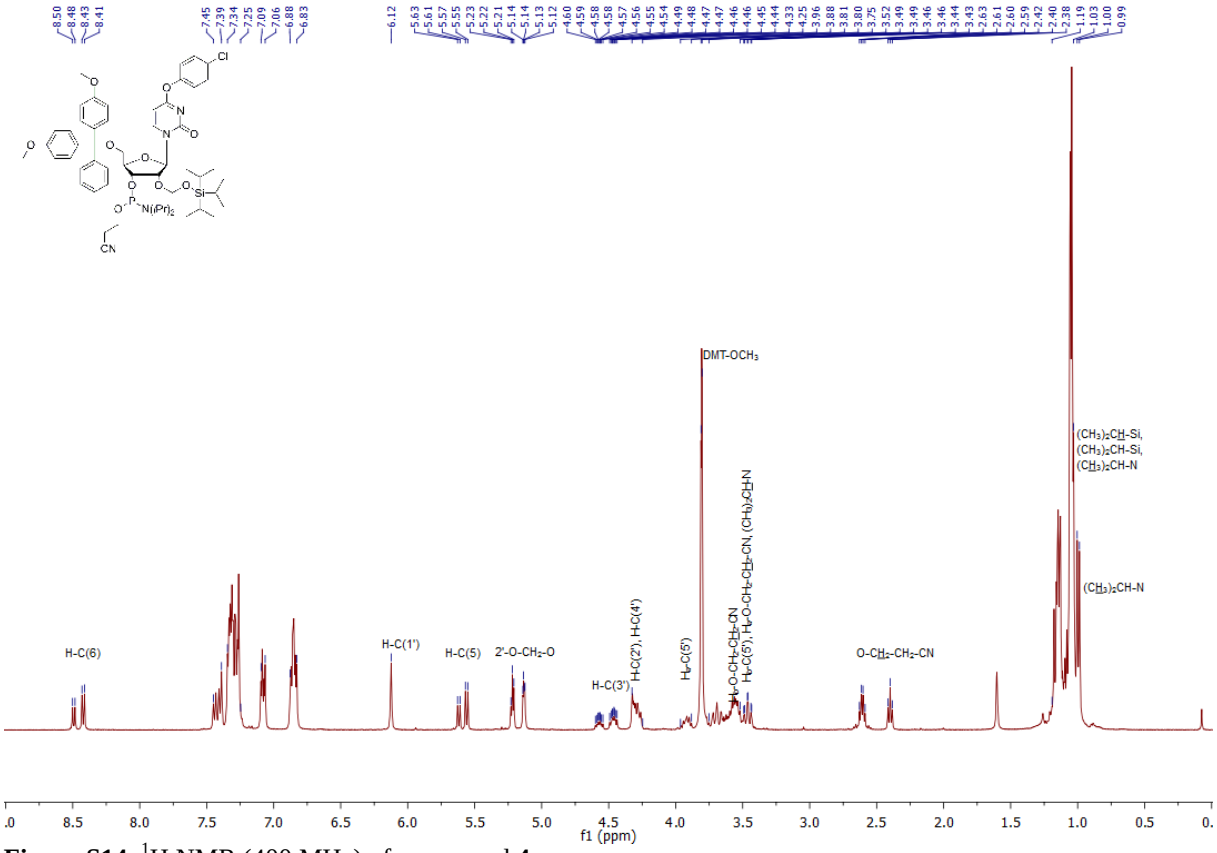

Figure S14. ^{1}H NMR (400 MHz) of compound **4**.

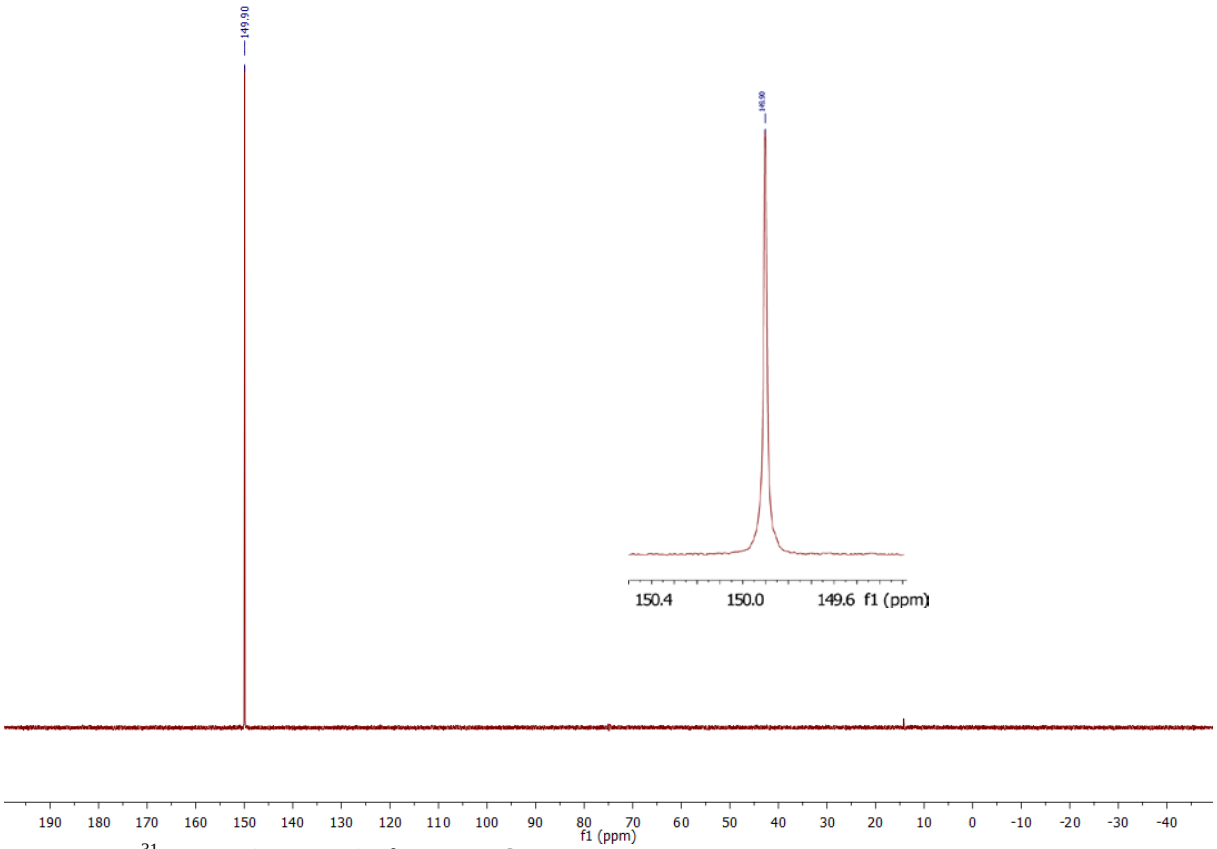

Figure S15. ^{31}P NMR (162 MHz) of compound **4**.

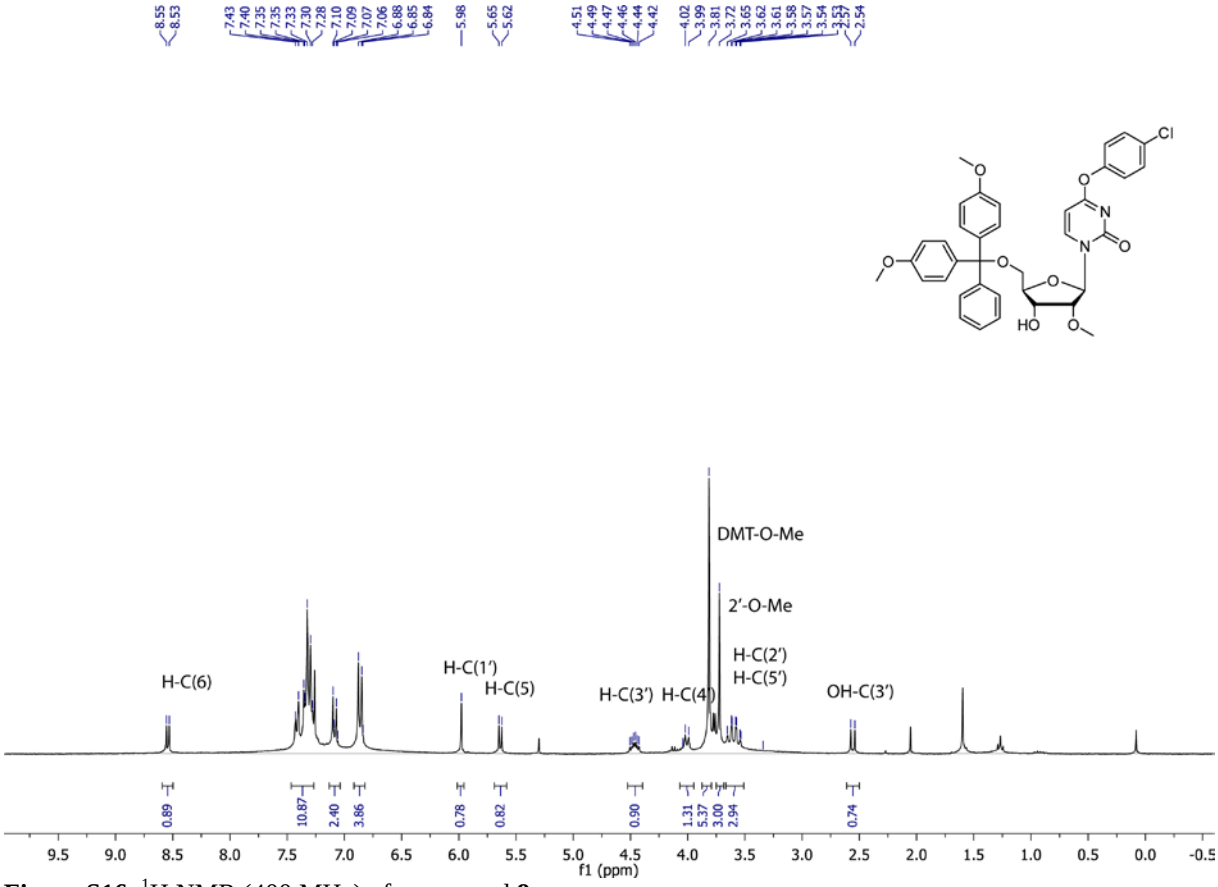

Figure S16. ^{1}H NMR (400 MHz) of compound **8**.

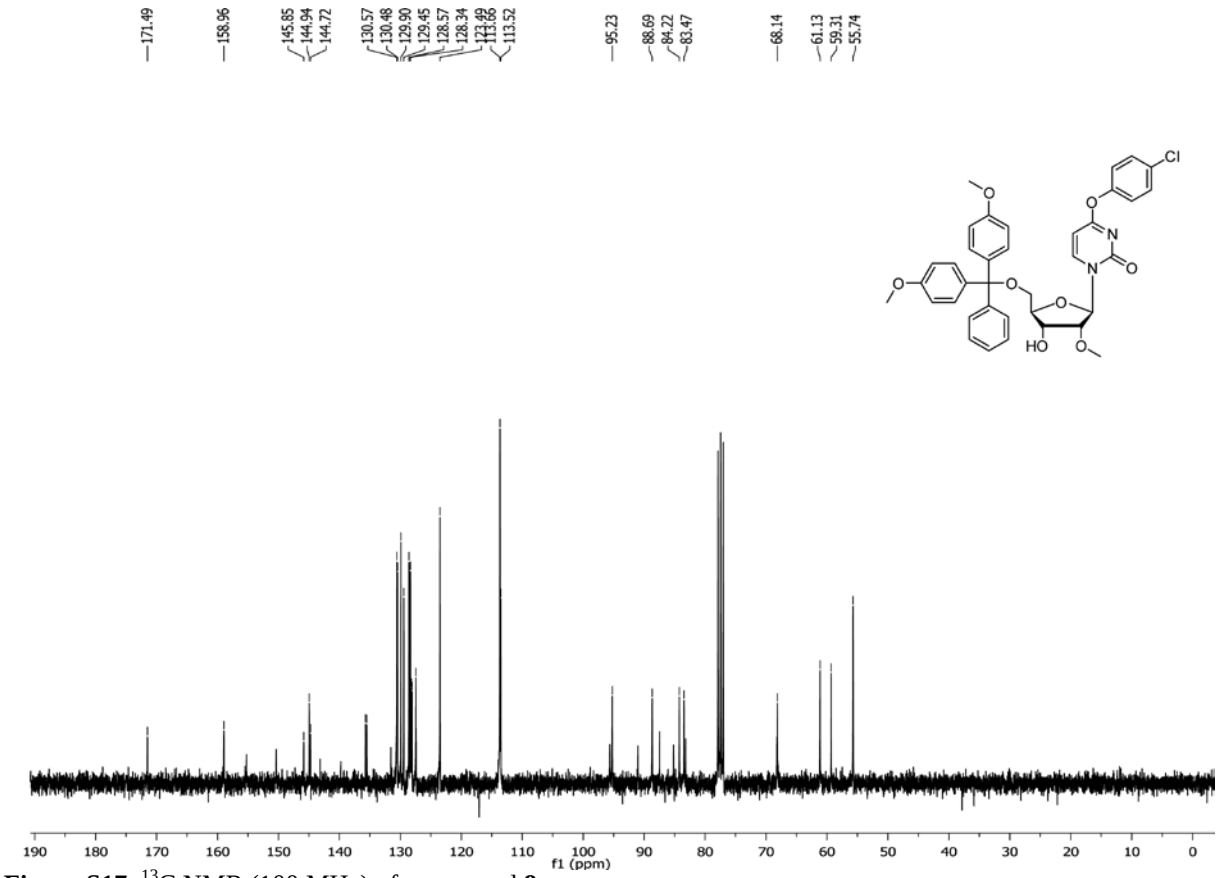

Figure S17. ^{13}C NMR (100 MHz) of compound **8**.

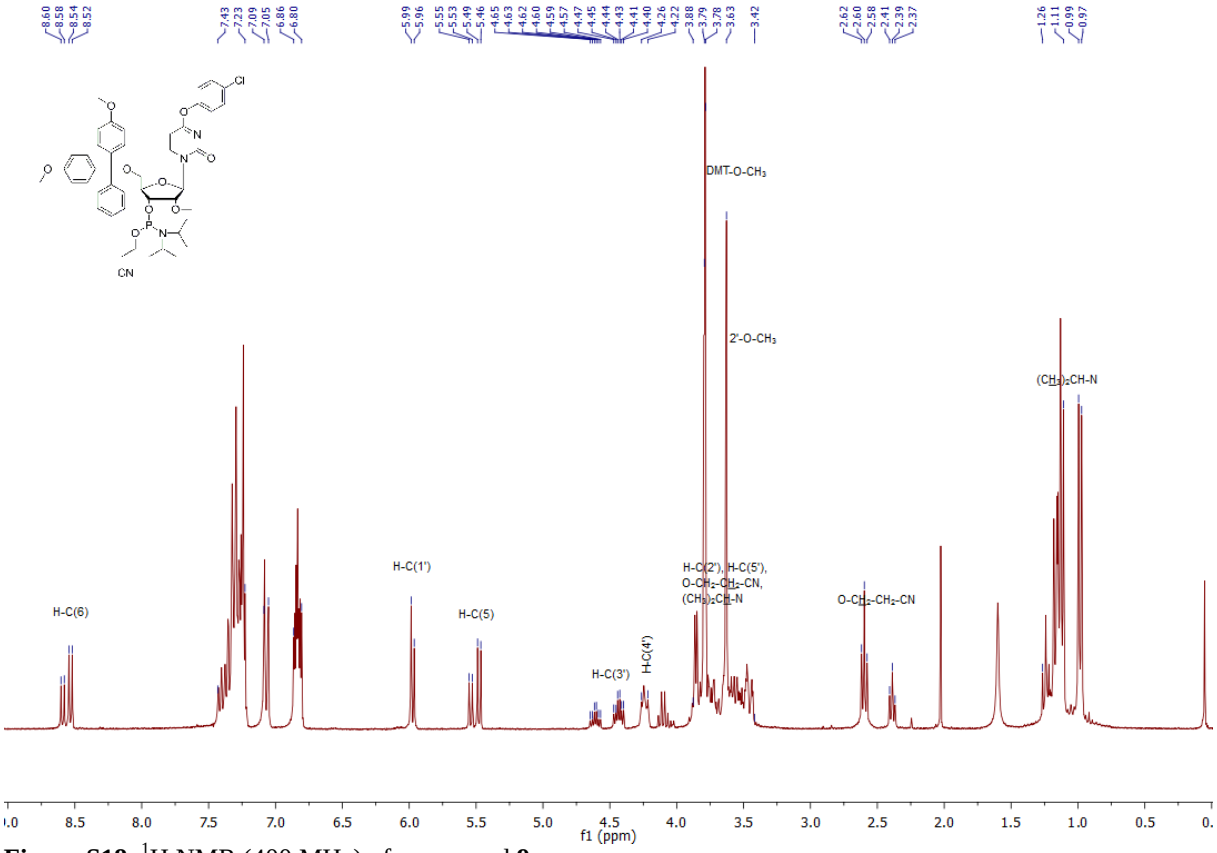

Figure S18. ^{1}H NMR (400 MHz) of compound **9**.

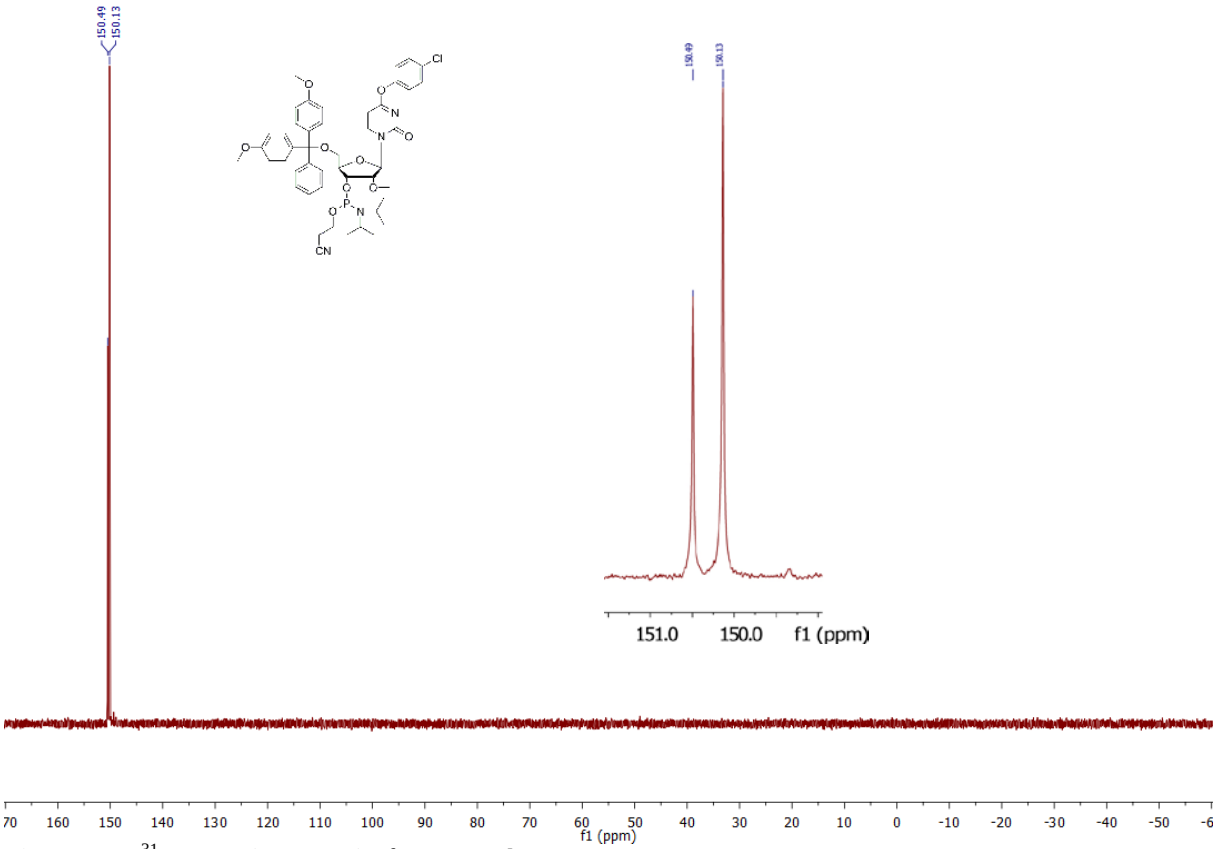

Figure S19. ^{31}P NMR (162 MHz) of compound **9**.